Influence of *N* doping on the Rashba coefficient, semiconductor-metal transition, and electron effective mass in $InSb_{1-x}N_x$ nanowires: Ten-band k·p model

X. W. Zhang,[1,2] W. J. Fan,[1,*] S. S. Li,[2] and J. B. Xia[2]
[1]*School of Electrical and Electronic Engineering, Nanyang Technological University, Singapore 639798, Singapore*
[2]*Institute of Semiconductors, Chinese Academy of Sciences, P.O. Box 912, Beijing 100083, China*
(Received 24 January 2007; published 22 May 2007)

The electronic structures of $InSb_{1-x}N_x$ nanowires are investigated using the ten-band $\mathbf{k}\cdot\mathbf{p}$ method. It is found that nitrogen increases the Rashba coefficient of the nanowires dramatically. For thick nanowires, the Rashba coefficient may increase by more than 20 times. The semiconductor-metal transition occurs more easily in $InSb_{1-x}N_x$ nanowires than in InSb nanowires. The electronic structure of $InSb_{1-x}N_x$ nanowires is very different from that of the bulk material. For fixed x the bulk material is a semimetal, while the nanowires are metal-like. In $InSb_{1-x}N_x$ bulk material and thick nanowires, an interesting decrease of electron effective mass is observed near $k=0$ which is induced by the nitrogen, but this phenomenon disappears in thin nanowires.

DOI: 10.1103/PhysRevB.75.205331 PACS number(s): 73.21.Hb, 73.63.Nm, 71.55.Eq, 71.70.Ej

I. INTRODUCTION

Dilute nitride alloys of III-V semiconductors have progressed rapidly over recent years following the discovery of strong negative band gap bowing effects.[1–4] Most theoretical and experimental work have concentrated on the alloys of $In_yGa_{1-y}As_{1-x}N_x$,[1,3–8] owing to its technological importance for fiber-optic communications at wavelengths of 1.3 and 1.55 μm. It is believed that nitrogen increases the electron effective mass of semiconductors,[9] while a first-principles calculation[10] shows that nitrogen decreases the electron effective mass near $k=0$. There are many investigations on narrow-gap $InSb_{1-x}N_x$ alloys.[11–17] The band gap of $InSb_{1-x}N_x$ can be tuned to be near zero, even negative,[16] by increasing the percentage of nitrogen. Therefore, the $InSb_{1-x}N_x$ might provide an alternative material, for infrared and terahertz applications, which would overcome some of the limitations of the more established materials.

Semiconductor nanowires can be grown out of numerous materials including InSb (Refs. 18 and 19) in a large range of radius by several methods. There is an increasing interest in the Rashba spin-orbit interaction[20–23] induced by an external electric field in semiconductor nanostructures because of its potential applications in spintronic devices. In two-dimensional semiconductor, it is found that the Rashba spin splitting exhibits a nonlinear behavior as a function of in-plane momentum,[24–30] and a two-parameter nonlinear Rashba model has been proposed by Yang and Chang,[31] which works well in describing this nonlinearity. Rashba spin splitting was measured in semiconductor nanowires.[21] Spin-polarized transport in semiconductor nanostructures is affected by Rashba spin-orbit interaction.[32,33] Many methods to synthesize diluted nitride semiconductor nanowires have been recently reported.[34,35] However, the electronic structure and the effect of the electric field, especially the Rashba spin-orbit splitting and the transport property, of diluted nitride semiconductor nanowires have not been studied.

In this paper, we calculate the electronic structures of $InSb_{1-x}N_x$ nanowires using the ten-band $\mathbf{k}\cdot\mathbf{p}$ method. The calculation model is given in Sec. II. Our numerical results and discussions are given in Sec. III. Our conclusions are presented in Sec. IV.

II. THEORY MODEL AND CALCULATIONS

We represent the ten-band Hamiltonian in the basis functions $|S_N\rangle\uparrow$, $|S\rangle\uparrow$, $|11\rangle\uparrow$, $|10\rangle\uparrow$, $|1-1\rangle\uparrow$, $|S_N\rangle\downarrow$, $|S\rangle\downarrow$, $|11\rangle\downarrow$, $|10\rangle\downarrow$, and $|1-1\rangle\downarrow$ as

$$H_{ten}=\begin{pmatrix} H_{five} & \\ & H_{five}\end{pmatrix}+H_{so}+V, \tag{1}$$

where $|S_N\rangle$ is the basis function of the N, H_{so} is the valence-band (VB) spin-orbit coupling Hamiltonian and is shown above,[22] and V is the electric-field potential term. H_{five} is written as

$$H_{five}=\begin{pmatrix} E_N & V_{NC}x^{1/2} & & & & \\ V_{NC}x^{1/2} & E_g & \frac{i}{\sqrt{2}}p_0k_+ & ip_0k_z & \frac{i}{\sqrt{2}}p_0k_- & \\ & -\frac{i}{\sqrt{2}}p_0k_- & & & & \\ & -ip_0k_z & & & & \\ & -\frac{i}{\sqrt{2}}p_0k_+ & & & & \end{pmatrix}+\begin{pmatrix} 0 & \\ & H_{k2}\end{pmatrix}, \tag{2}$$

where E_g is the band gap of bulk material, $p_0=\hbar\sqrt{\frac{E_P}{2m_0}}$, E_p is the matrix element of Kane's theory, $k_\pm=k_x\pm ik_y$, k is the wave vector, $E_N=0.65$ eV is the nitrogen energy level relative to the valence-band maximum, $V_{NC}=3.0$ eV is the coupling strength between the conduction band (CB) state and the nitrogen state,[36] and x is the composition of the N. H_{k2} is a 4×4 matrix which is written as

$$H_{k2}=\frac{\hbar^2}{2m_0}\begin{pmatrix} P_e & 0 & 0 & 0\\ 0 & -P_1 & -G & -F\\ 0 & -G^\star & -P_3 & -G\\ 0 & -F^\star & -G^\star & -P_1\end{pmatrix}, \tag{3}$$

where

TABLE I. The parameters of InSb material.

m_c	L	M	N	E_P (eV)	E_g (eV)	Δ_{so} (eV)	ϵ_r
$0.0136m_0$	98.9	4.58	101.0	21.2	0.2352	0.81	16.8

$$P_e = \gamma_c k_- k_+ + \gamma_c k_z^2, \tag{4a}$$

$$P_1 = \frac{L' + M'}{2} k_- k_+ + M' k_z^2, \tag{4b}$$

$$P_3 = M' k_- k_+ + L' k_z^2, \tag{4c}$$

$$F = \frac{L' - M' - N'}{4} k_+^2 + \frac{L' - M' + N'}{4} k_-^2, \tag{4d}$$

$$F^* = \frac{L' - M' - N'}{4} k_-^2 + \frac{L' - M' + N'}{4} k_+^2, \tag{4e}$$

$$G = \frac{1}{\sqrt{2}} N' k_- k_z, \tag{4f}$$

$$G^* = \frac{1}{\sqrt{2}} N' k_+ k_z. \tag{4g}$$

γ_c, L', M', and N' are given by

$$\gamma_c = \frac{m_0}{m_c} - \frac{E_p}{3}\left(\frac{2}{E_g} + \frac{1}{E_g + 3\lambda}\right), \tag{5a}$$

$$L' = L - E_p/E_g, \tag{5b}$$

$$M' = M, \tag{5c}$$

$$N' = N - E_p/E_g, \tag{5d}$$

where m_c is the electron effective mass, L, M, and N are the Luttinger parameters, and $\lambda = \Delta_{so}/3$, with Δ_{so} the spin-orbit splitting energy at $k=0$ of VB.[22]

We assume that the nanowires have cylindrical symmetry, the longitudinal axis is along the z direction, and the electric field is applied along the x direction (i.e., $\mathbf{F} = F\hat{\mathbf{x}}$, where F is the field strength in the nanowires). So the electric-field potential term can be written as

$$V = eFx = eFr(e^{i\theta} + e^{-i\theta}), \tag{6}$$

where (r, θ) is the polar coordinate system. It is noticed that due to the dielectric effect, the electric field in the nanowires has the following relationship with the external electric field:

$$\mathbf{F} = \frac{2\epsilon_0}{\epsilon_r + \epsilon_0} \mathbf{F}_{ext}, \tag{7}$$

where ϵ_r and ϵ_0 are the dielectric constants inside and outside the nanowires, respectively.

We assume that the electrons and holes are confined laterally in an infinitely high potential barrier. The lateral wave function is expanded in Bessel functions and the longitudinal wave function is the plane wave. The total envelope function including the electron and hole states is

$$\Psi_{J,k_z} = \sum_n \begin{pmatrix} f_{l,n,\uparrow} A_{l,n} J_l(k_n^l r) e^{il\theta} \\ e_{l,n,\uparrow} A_{l,n} J_l(k_n^l r) e^{il\theta} \\ b_{l-1,n,\uparrow} A_{l-1,n} J_{l-1}(k_n^{l-1} r) e^{i(l-1)\theta} \\ c_{l,n,\uparrow} A_{l,n} J_l(k_n^l r) e^{il\theta} \\ d_{l+1,n,\uparrow} A_{l+1,n} J_{l+1}(k_n^{l+1} r) e^{i(l+1)\theta} \\ f_{l+1,n,\downarrow} A_{l+1,n} J_{l+1}(k_n^{l+1} r) e^{i(l+1)\theta} \\ e_{l+1,n,\downarrow} A_{l+1,n} J_{l+1}(k_n^{l+1} r) e^{i(l+1)\theta} \\ b_{l,n,\downarrow} A_{l,n} J_L(k_n^l r) e^{il\theta} \\ c_{l+1,n,\downarrow} A_{l+1,n} J_{l+1}(k_n^{l+1} r) e^{i(l+1)\theta} \\ d_{l+2,n,\downarrow} A_{l+2,n} J_{l+2}(k_n^{l+2} r) e^{i(l+2)\theta} \end{pmatrix} e^{ik_z z}, \tag{8}$$

where $J = l + 1/2$ is the total angular momentum and $A_{l,n}$ is the normalization constant,

$$A_{l,n} = \frac{1}{\sqrt{\pi} R J_{l+1}(\alpha_n^l)}, \tag{9}$$

with α_n^l the nth zero point of the Bessel function $J_l(x)$.

III. RESULTS AND DISCUSSION

The parameters of the InSb material used in this paper are listed in Table I. However, these parameters measured in the bulk material include some contributions from, for example, the nonlocal character of the self-consistent potential that are absent in narrow-gap nanostructures.[37] Therefore, using these parameters requires taking special precautions. The nonlocal contributions are

$$\Delta L = -21\delta_{nl}, \quad \Delta M = 3\delta_{nl}, \quad \Delta N = -24\delta_{nl}, \quad \Delta\alpha = -10\delta_{nl}, \tag{10}$$

$$\delta_{nl} = \frac{2}{15\pi\epsilon_r E_g}\sqrt{\frac{E_B E_p}{3}}, \tag{11}$$

where $E_B = 27.211$ eV.

The energy levels of the $InSb_{1-x}N_x$ nanowires with $R = 20$ nm and $x = 0.01$ at $F = 0.5$ mV/nm as functions of k_z are shown in Fig. 1(a). We find that the band gap is about 120 meV, and 1% of nitrogen can decrease the band gap by more than 100 meV. Transverse electric field brings inversion asymmetry along its direction and thus introduces the Rashba spin-orbit coupling. All the spin degenerate bands are split when $k_z \neq 0$ in Fig. 1(a). The Rashba splitting energy of the lowest two CBs is shown in Fig. 1(b). The splitting in-

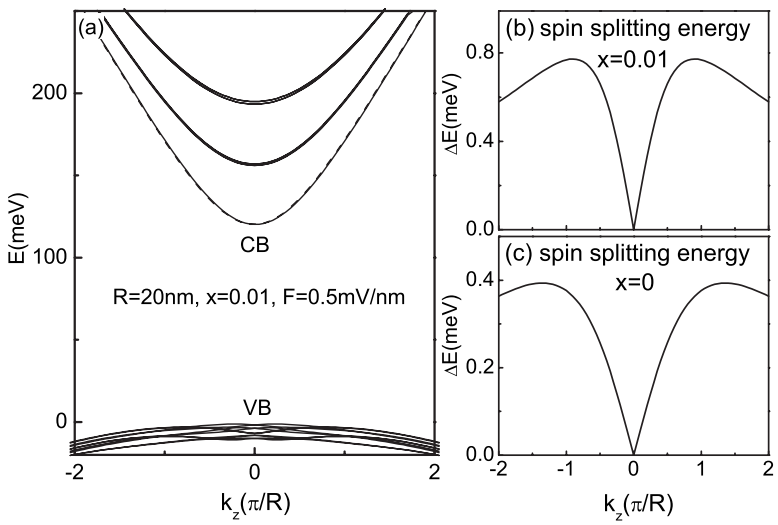

FIG. 1. (a) Energy levels of $InSb_{1-x}N_x$ nanowires with $R=20$ nm and $x=0.01$ at $F=0.5$ mV/nm as functions of k_z. (b) Rashba splitting energy of the lowest two CBs in the $x=0.01$ case. (c) Rashba splitting energy of the lowest two CBs in the $x=0$ case.

creases linearly with k_z when k_z is small, then decreases with k_z when k_z is large, because the CBs become far away from the VBs and the Rashba splitting of the CBs comes from its coupling with the VBs.[30] Recently, Yang and Chang have found that the Rashba spin splitting is intrinsically a nonlinear function of the momentum, and the linear Rashba model may overestimate it significantly, especially in narrow-gap semiconductors.[30,31] Their two-parameter nonlinear Rashba model[31] is confirmed in $InSb_{1-x}N_x$ nanowires as well as in InSb nanowires, as shown in Fig. 1(c). We find that the nonlinear Rashba effect is more explicit in Fig. 1(b) than in Fig. 1(c), with the maximum appearing at a smaller wave vector. The reason is the decrease of band gap induced by nitrogen.

However, the linear relationship[20] still remains near $k_z=0$, so we can define a Rashba coefficient as $\alpha=\frac{1}{2}\frac{\partial\Delta E}{\partial k_z}\big|_{k_z=0}$.

Figure 2 shows the Rashba coefficient as a function of R and x. We find that when $x=0$, the Rashba coefficient increases with the radius and then saturates, which is in agreement with the previous result and the deduced formula[22,30]

$$\alpha=\frac{\hbar^2}{2m_0}E_p\frac{\lambda(2E_g'+3\lambda)}{E_g'^2(E_g'+3\lambda)^2}eF, \tag{12}$$

where E_g' is the band gap of the $InSb_{1-x}N_x$ wire. When the nitrogen composition increases, the Rashba coefficient increases. The reason is that as x increases, E_g' decreases, so the coupling between CB and VB becomes strong. When R is larger, the relative increase of the Rashba coefficient with x is larger. This is because when R is larger, the band gap of InSb nanowires E_{g0}' is smaller, and the relative decrease of band gap $(E_{g0}'-E_g')/E_{g0}'$ is larger for a given x. The Rashba coefficient can increase by more than 20 times as x increases.

From Eq. (12), we find that the Rashba coefficient increases with the electric field F. On the other hand, in the case of a large electric field [see Fig. 3(a)], the CBs and VBs overlap, and the Rashba splitting of the lowest CBs does not exist. In this case, there is another interesting phenomenon. Because the intrinsic Fermi level (dashed line) crosses with

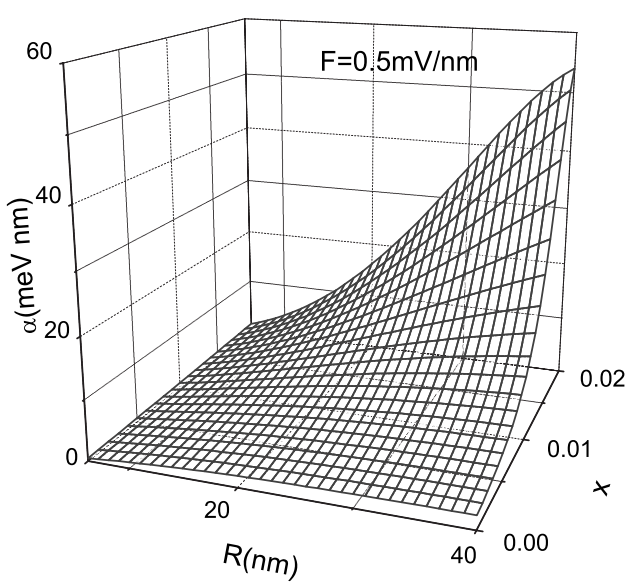

FIG. 2. (a) Rashba coefficient of $InSb_{1-x}N_x$ nanowires at $F=0.5$ mV/nm as a function of R and x.

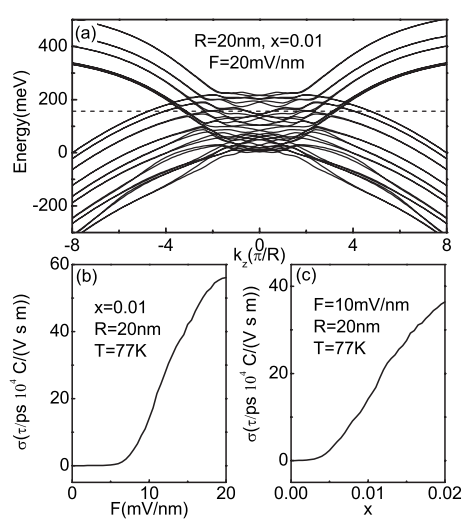

FIG. 3. (a) Energy levels of $InSb_{1-x}N_x$ nanowires with $R=20$ nm and $x=0.01$ at $F=20$ mV/nm as functions of k_z. (b) Conductivity of the $InSb_{1-x}N_x$ nanowires with $R=20$ nm and $x=0.01$ at $T=77$ K as a function of F. (c) Conductivity at $F=10$ mV/nm and $T=77$ K as a function of x.

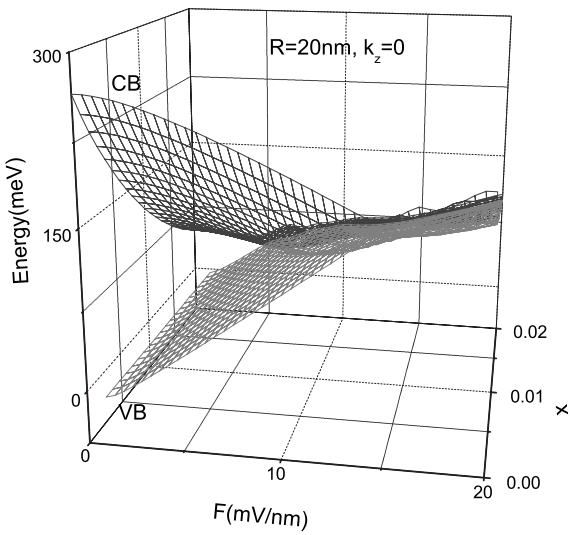

FIG. 4. Lowest CB and highest VB energy levels at $k_z=0$ of $InSb_{1-x}N_x$ nanowires with $R=20$ nm as functions of F and x.

many bands, there are many carriers on the Fermi level which contribute to the conductivity of the nanowires along the wire direction.

We calculate the conductivity of the nanowires along the wire direction using the Boltzmann equation and the relaxation-time approximation, assuming that the momentum relaxation time (τ) is energy independent,[23,38]

$$\sigma = \frac{e^2\tau}{2\pi^2R^2\hbar^2k_BT}\sum_i \int \left(\frac{\partial E_i}{\partial k_z}\right)^2 \frac{e^{(E_i-E_F)/k_BT}}{(1+e^{(E_i-E_F)/k_BT})^2}dk_z, \quad (13)$$

where i refers to different energy bands.

The conductivity of $InSb_{1-x}N_x$ nanowires with $R=20$ nm and $x=0.01$ at 77 K as a function of the electric field is shown in Fig. 3(b). When F is smaller than 6 mV/nm, the conductivity is zero and there will not be electric current in the intrinsic nanowires. When F is larger than 6 mV/nm, the conductivity increases dramatically with F. When $F=20$ mV/nm, the conductivity has the magnitude of metal conductivity, so the wire is transformed from a semiconductor into a metal. Unlike the traditional transistor, we can use the intrinsic nanowires to design a different kind of quantum transistors, which can be turned on and switched off by a transverse electric field. Figure 3(c) shows that the conductivity at given R and F increases with x.

The lowest CB and highest VB energy levels at $k_z=0$ of $InSb_{1-x}N_x$ nanowires with $R=20$ nm as functions of F and x are shown in Fig. 4. Actually, they are correctly named only when the CB is above the VB. From the figure, we find that when $x=0$, the band gap at $F=0$ is about 270 meV, and an electric field of about 14 mV/nm can make the bands overlap, and we named this electric field as the critical electric field. As x increases, a smaller electric field can make the bands overlap, i.e., the critical electric field decreases. When $x=0.02$, the critical electric field is about 5 mV/nm.

When x is larger than a critical value of about 0.017, the bulk $InSb_{1-x}N_x$ has negative band gap, as shown in Fig. 5(a). In calculating the electronic structure of bulk material, we have expanded the wave function in plane waves and have used the k_z and $k_\pm$ in the Hamiltonian [Eq. (1)] as good quantum numbers. When $x>0.017$, the bulk $InSb_{1-x}N_x$ has semimetallic band structure. From Figs. 5(b) and 5(c), we find that the light-hole and heavy-hole bands are near the Fermi level (dashed line), and the CB is below them. It is noticed that at the Fermi level, the light-hole and heavy-hole bands are tangential to each other, so the conductivity is zero at zero temperature, which can be large at nonzero temperatures. From Fig. 5(d), we find that the nitrogen almost does not change the VBs of nanowires and reduces the CBs with increasing x, which is similar to the bulk material case. How-

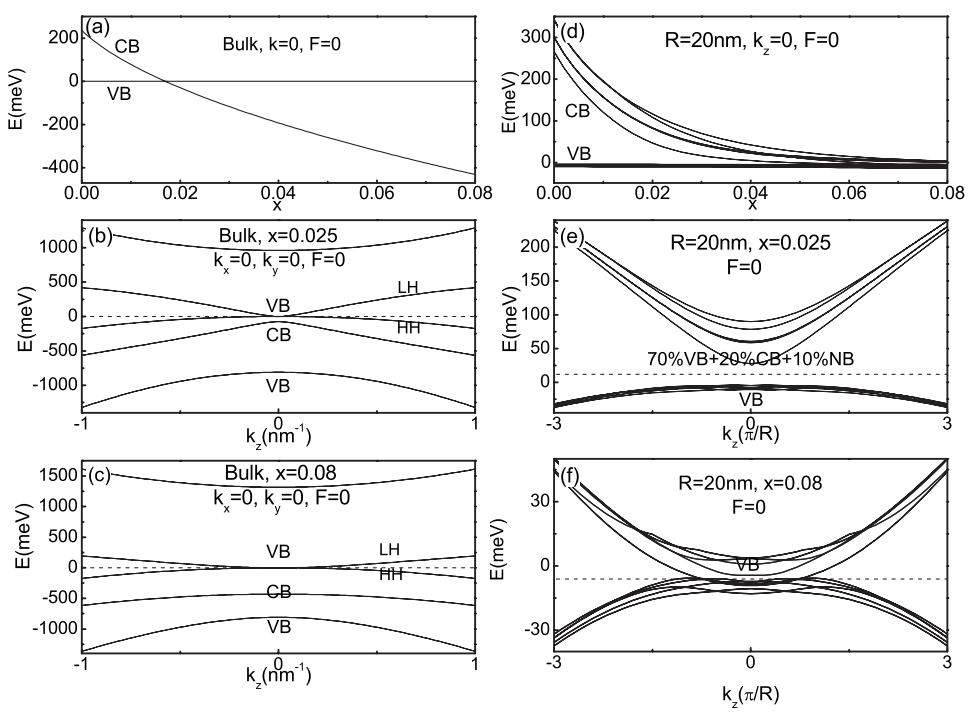

FIG. 5. Electronic structures of $InSb_{1-x}N_x$ bulk material and nanowires. (a) Bulk, $\mathbf{k}=0$, and $F=0$ as functions of x. (b) Bulk, $x=0.025$, $k_x=0$, $k_y=0$, and $F=0$ as functions of k_z. (c) Similar to (b) but for $x=0.08$. (d) Nanowire, $R=20$ nm, $k_z=0$, and $F=0$ as functions of x. (e) Nanowire, $R=20$ nm, $x=0.025$, and $F=0$ as functions of k_z. (f) Similar to (e) but for $x=0.08$.

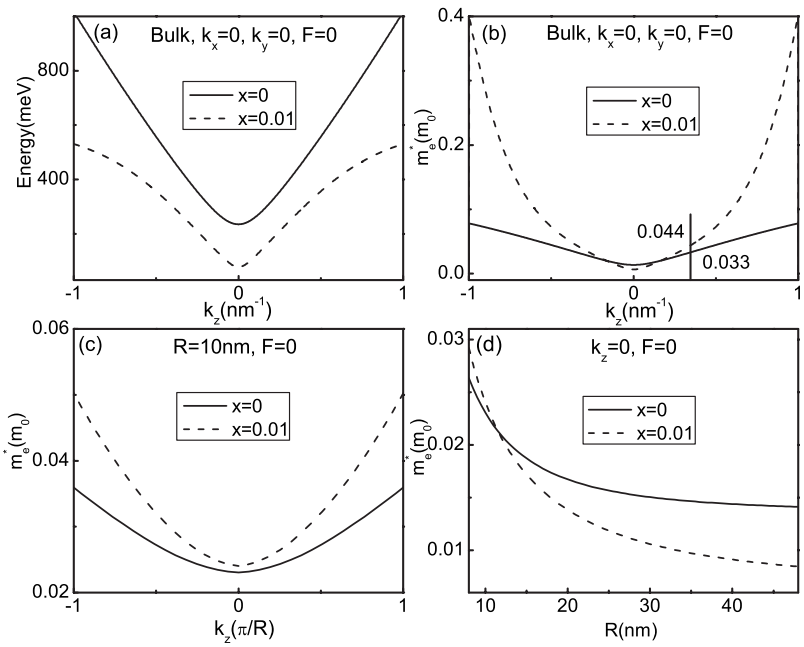

FIG. 6. (a) CBs of $InSb_{1-x}N_x$ bulk material at $k_x=0$, $k_y=0$, and $F=0$ as functions of k_z. (b) Electron effective masses of $InSb_{1-x}N_x$ bulk material at $k_x=0$, $k_y=0$, and $F=0$ as functions of k_z. (c) Electron effective masses of $InSb_{1-x}N_x$ nanowires with $R=10$ nm at $F=0$ as functions of k_z. (d) Electron effective masses of $InSb_{1-x}N_x$ nanowires at $k_z=0$ and $F=0$ as functions of R.

ever, the CBs come close to the VBs at a larger x compared to the bulk material because the quantum confinement effect increases the band gap. The energy bands of $InSb_{1-x}N_x$ nanowires with $R=20$ nm and $F=0$ at $x=0.025$ and 0.08 are shown in Figs. 5(e) and 5(f), respectively. At $x=0.025$, the lowest CB is about 33 meV above the highest VB, and the nanowire is still a semiconductor, though the lowest band above the Fermi level contains 70% VB, 20% CB state, 10% nitrogen state components. At $x=0.08$, similar to the bulk material, the nanowire is not a semiconductor and the bands near the Fermi level are VBs. Compared with Fig. 5(c), the Fermi level in Fig. 5(f) crosses with some bands and the nanowire has nonzero conductivity at zero temperature. Thus, the nanowire is metal-like, which is different from what is observed in the bulk material. This is because in nanowires there is an additional coupling between the bands due to the lateral quantum confinement which interacts with the coupling of k_z terms, leading to the complex metal-like electronic structure.

The electron effective mass of $InSb_{1-x}N_x$ bulk material has been widely measured.[11–14] It is believed that the electron effective mass at the Fermi level increases with the nitrogen composition; for example, Murdin *et al.*[12] found that 1% of nitrogen can increase the electron effective mass at the Fermi level from 0.033 to 0.044. It is obvious that 0.033 is not the mass of InSb at $k=0$ (0.0136), but rather the mass at the wave vector on the Fermi surface. We calculate the CBs and electron effective masses of $InSb_{1-x}N_x$ bulk material using the formula $1/m_e^*=|\partial E_e(k)/\partial k|/\hbar^2 k$,[9] which are shown in Figs. 6(a) and 6(b), respectively. We find in Fig. 6(b) that when k is far away from 0, the mass increases with the nitrogen composition, and at $k_F=0.35$ nm^{-1}, 1% of nitrogen can increase the mass from 0.033 to 0.044, which is in agreement with the experimental result.[12] On the other hand, the electron effective mass of $InSb_{1-x}N_x$ bulk material near $k=0$ decreases with the nitrogen composition. Nitrogen has two effects on the electron effective mass. One is the direct effect in which nitrogen increases the mass, which has been discussed thoroughly before.[9] The other is the indirect effect where nitrogen decreases the band gap, pushing the CB to the VB and strengthening the coupling between CB and VB, so as to decrease the mass. In narrow-gap semiconductors, the indirect effect may dominate near $k=0$. Previous works[7,9] show that in wide-gap semiconductors, the indirect effect is small and the direct effect always dominates so the electron effective masses always increase with nitrogen composition. We show the electron effective masses of $InSb_{1-x}N_x$ nanowires with $R=10$ nm at $F=0$ as functions of k_z in Fig. 6(c). We find that at any k_z, the electron effective mass increases with x, which is similar with the wide-gap semiconductor case,[7,9] because the band gap of the thin $InSb_{1-x}N_x$ nanowires is large. The phenomenon of nitrogen decreasing the electron effective mass at $k_z=0$ disappears in thin $InSb_{1-x}N_x$ nanowires but appears in thick $InSb_{1-x}N_x$ nanowires, as shown in Fig. 6(d).

IV. CONCLUSIONS

The electronic structures of $InSb_{1-x}N_x$ nanowires are investigated by using the ten-band $\mathbf{k}\cdot\mathbf{p}$ method. The $InSb_{1-x}N_x$ nanowires exhibit extremely strong band-gap bowing with the nitrogen composition x. It is found that nitrogen increases the Rashba coefficient of the nanowires dramatically. For thick nanowires, the Rashba coefficient may increase by more than 20 times. The interesting nonlinear Rashba effect[30,31] is more explicit in diluted nitride semiconductors. The semiconductor-metal transition occurs more easily in $InSb_{1-x}N_x$ nanowires than in InSb nanowires. The semiconductor-metal transition of $InSb_{1-x}N_x$ nanowires can be used to design a different kind of quantum transistor. The electronic structure of $InSb_{1-x}N_x$ nanowires is different from that of the bulk material. For a fixed x the bulk material is a semimetal, whereas the nanowires are metal-like. In

$InSb_{1-x}N_x$ bulk material and thick nanowires, the electron effective mass near $k=0$ decreases with x.

ACKNOWLEDGMENTS

W.J.F. would like to acknowledge the support from A^*STAR (Grant No. 0421010077). J.B.X. and S.S.L. would like to acknowledge the support from the National Natural Science Foundation of China, Grants No. 90301007, No. 60521001, and No. 60325416. X.W.Z. would like to thank Kai Chang and W. Yang for their help on Rashba spin-orbit effect.

*Electronic address: ewjfan@ntu.edu.sg

[1] W. Shan, W. Walukiewicz, J. W. Ager III, E. E. Haller, J. F. Geisz, D. J. Friedman, J. M. Olson, and S. R. Kurtz, Phys. Rev. Lett. **82**, 1221 (1999).
[2] A. Lindsay, S. Tomić, and E. P. O'Reilly, Solid-State Electron. **47**, 443 (2003).
[3] Stanko Tomić, Eoin P. O'Reilly, Peter J. Klar, Heiko Grűuning, Wolfram Heimbrodt, Weimin M. Chen, and Irina A. Buyanova, Phys. Rev. B **69**, 245305 (2004).
[4] Stanko Tomić, Phys. Rev. B **73**, 125348 (2006).
[5] S. T. Ng, W. J. Fan, Y. X. Dang, and S. F. Yoon, Phys. Rev. B **72**, 115341 (2005).
[6] Y. X. Dang, W. J. Fan, S. T. Ng, S. Wicaksono, S. F. Yoon, and D. H. Zhang, J. Appl. Phys. **98**, 026102 (2005).
[7] Seth R. Bank, Homan B. Yuen, Mark A. Wistey, Vincenzo Lordi, Hopil P. Bae, and James S. Harris, Jr., Appl. Phys. Lett. **87**, 021908 (2005).
[8] L. H. Li, V. Sallet, G. Patriarche, L. Largeau, S. Bouchoule, L. Travers, and J. C. Harmand, Appl. Phys. Lett. **83**, 1298 (2003).
[9] Czeslaw Skierbiszewski, Semicond. Sci. Technol. **17**, 803 (2002).
[10] I. Gorczyca, C. Skierbiszewski, T. Suski, N. E. Christensen, and A. Svane, Phys. Rev. B **66**, 081106(R) (2002).
[11] B. N. Murdin, M. Kamal-Saadi, A. Lindsay, E. P. O'Reilly, A. R. Adams, G. J. Nott, J. G. Crowder, C. R. Pidgeon, I. V. Bradley, J.-P. R. Wells, T. Burke, A. D. Johnson, and T. Ashley, Appl. Phys. Lett. **78**, 1568 (2001).
[12] B. N. Murdin, A. R. Adams, P. Murzyn, C. R. Pidgeon, I. V. Bradley, J.-P. R. Wells, Y. H. Matsuda, N. Miura, T. Burke, and A. D. Johnson, Appl. Phys. Lett. **81**, 256 (2002).
[13] T. D. Veal, I. Mahboob, C. F. McConville, T. M. Burke, and T. Ashley, Appl. Phys. Lett. **83**, 1776 (2003).
[14] I. Mahboob, T. D. Veal, and C. F. McConville, Appl. Phys. Lett. **83**, 2169 (2003).
[15] T. Ashley, T. M. Burke, G. J. Pryce, A. R. Adams, A. Andreev, B. N. Murdin, E. P. O'Reilly, and C. R. Pidgeon, Solid-State Electron. **47**, 387 (2003).
[16] T. D. Veal, I. Mahboob, and C. F. McConville, Phys. Rev. Lett. **92**, 136801 (2004).
[17] T. D. Veal, I. Mahboob, L. F. J. Piper, T. Ashley, M. Hopkinson, and C. F. McConville, J. Phys.: Condens. Matter **16**, S3201 (2004).
[18] N. Mingo, Appl. Phys. Lett. **84**, 2652 (2004).
[19] S. V. Zaitsev-Zotov, Yu. A. Kumzerov, Yu. A. Firsov, and P. Monceau, Journal of Experimental and Theoretical Physics Letters **77**, 135 (2003).
[20] E. I. Rashba, Sov. Phys. Solid State **2**, 1109 (1960).
[21] V. A. Guzenko, J. Knobbe, H. Hardtdegen, Th. Schäpers, and A. Bringer, Appl. Phys. Lett. **88**, 032102 (2006).
[22] X. W. Zhang and J. B. Xia, Phys. Rev. B **74**, 075304 (2006).
[23] X. W. Zhang, S. S. Li, and J. B. Xia, Appl. Phys. Lett. **89**, 172113 (2006).
[24] R. Winkler and U. Rőssler, Phys. Rev. B **48**, 8918 (1993).
[25] E. A. de Andrada e Silva, G. C. La Rocca, and F. Bassani, Phys. Rev. B **50**, 8523 (1994).
[26] E. A. de Andrada e Silva, G. C. La Rocca, and F. Bassani, Phys. Rev. B **55**, 16293 (1997).
[27] R. Winkler, Phys. Rev. B **62**, 4245 (2000).
[28] Saadi Lamari, Phys. Rev. B **64**, 245340 (2001).
[29] X. Cartoixa, L. W. Wang, D. Z.-Y. Ting, and Y. C. Chang, Phys. Rev. B **73**, 205341 (2006).
[30] W. Yang and Kai Chang, Phys. Rev. B **73**, 113303 (2006).
[31] W. Yang and Kai Chang, Phys. Rev. B **74**, 193314 (2006).
[32] L. G. Wang, Kai Chang, and K. S. Chan, J. Appl. Phys. **99**, 043701 (2006).
[33] W. Yang and Kai Chang, Phys. Rev. B **73**, 045303 (2006).
[34] Hee Won Seo, Seung Yong Bae, Jeunghee Park, Myungil Kang, and Sangsig Kim, Chem. Phys. Lett. **378**, 420 (2003).
[35] Y. P. Song, H. Z. Zhang, C. Lin, Y. W. Zhu, G. H. Li, F. H. Yang, and D. P. Yu, Phys. Rev. B **69**, 075304 (2004).
[36] I. Vurgaftman and J. R. Meyer, J. Appl. Phys. **94**, 3675 (2003).
[37] Al. L. Efros and M. Rosen, Phys. Rev. B **58**, 7120 (1998).
[38] N. W. Ashcroft and N. D. Mermin, *Solid State Physics* (Holt, Rinehart and Winston, New York, 1976).